dichotomy may still offer the explanation, if also the stabilities of the ion/molecule complexes, leading to either syn or anti elimination, are taken into account. In principle, these stabilities can be obtained by ab initio calculations.[15,16] However, this is beyond the scope of the present study. Therefore, rough approximations to the bond dissociation energies of the ion/molecule complexes have been obtained by calculating the pure long-range electrostatic interactions between the species,[57] estimating the geometric parameters from the corresponding molecular models. For **3a** these calculations clearly indicate that the formation of the complex leading to syn elimination can be as much as 10 kcal/mol more exothermic than the formation of the complex leading to anti elimination. Thus, in spite of the relatively low intrinsic reaction barrier, associated with the electronically favored anti elimination, the density of states in the transition state of the syn elimination may still be higher relative to the anti elimination. Consequently, solvated alkoxide formation is favored over free alkoxide formation as is visualized by the potential energy profile outlined in Figure 2.

For **3b** the approximations to the bond dissociation energies of the ion/molecule complexes, leading to either syn or anti elimination, suggest equal exothermicity with respect to the formation of both complexes. Since also both intrinsic reaction barriers of syn and anti elimination suffer about equally from the unfavorable geometry of the substrate, the preference for syn elimination, e.g., solvated alkoxide formation, may be lost. This is visualized by the potential energy profile outlined in Figure 3. In the proposed mechanism only a fraction of all the phase space of the ion/molecule complex is associated with the conversion into products. This fraction is related to the structure of the transition state, implying that collision dynamics may play an important role in the product distribution. The importance of collision dynamics in product distribution of gas-phase ion/molecule reactions has been suggested earlier by Minato and Yamabe on the basis of an ab initio study of the reaction of F^- and FC_2H_5 (vide supra).[16]

Still, our model is only based on branching ratios, disregarding the influence of minor changes in reaction energetics and reactant structure on the encounter rate itself, and the rate of nonreactive collisions.[58] We realize that this aspect of the mechanism must be investigated by analyzing the absolute kinetics of the elimination reactions of **3a** and **3b**. Unfortunately, absolute gas-phase rate constant measurements still suffer from large experimental errors, a consequence of which small changes in the absolute rates cannot be detected.

Conclusions

Although the energy profiles of ion/molecule reactions in the gas phase principally differ from those in the condensed phase, it seems that the properties of the transition state of base-induced gas-phase elimination reactions of ethers are very well in line with the theoretical model set up for concerted β-eliminations in the condensed phase. However, where in the condensed phase association of solvent molecules or counterions may play an important role, electrostatic interactions in the gas phase of the base and the substrate itself may partly be responsible for the mechanistic course of the elimination reaction.

Acknowledgment. We thank Mr. F. A. Pinkse for his expert technical assistance and the Netherlands Organization for Pure Research (SON/ZWO) for financial support.

Registry No. 3a, 15875-99-7; **3b**, 15876-31-0; Dz, 7782-39-0; diethyl ether, 60-29-7.

(57) (a) Grabowski, J. J.; DePuy, C. H.; Bierbaum, V. M. *J. Am. Chem. Soc.* **1983**, *105*, 2565. (b) Squires, R. R.; Bierbaum, V. M.; Grabowski, J. J.; DePuy, C. H. *Ibid.* **1983**, *105*, 5183. (c) Ingemann, S.; Nibbering N. M. M. *J. Org. Chem.* **1985**, *50*, 682. (d) Ausloos, P.; Lias, S. G. *J. Am. Chem. Soc.* **1981**, *103*, 3641. (e) Hunter, E. P.; Lias, S. G. *J. Phys. Chem.* **1982**, *86*, 2769.

(58) We thank one of the referees for bringing this point to our attention.

(59) Bartmess, J. E.; McIver, R. T. *Gas Phase Ion Chemistry*, Bowers, M. T.; Ed.; Academic Press: New York, 1979; Vol. 2, Chapter 11, p 87.

Ab Initio Study of the Unimolecular Pyrolysis Mechanisms of Formic Acid: Additional Comments Based on Refined Calculations

P. Ruelle

Contribution from the School of Pharmacy, University of Lausanne, CH-1005 Lausanne, Switzerland. *Received July 24, 1986*

Abstract: Refined ab initio calculations on the dehydration and decarboxylation mechanisms of formic acid in the gaseous state above 670 °C are presented, taking into account the effect of electron correlation on both the geometries and energies of the different stationary points. The classical barrier heights of the two processes are much more affected by the quality of the basis set used at the SCF level and by the correlation corrections evaluated in single-point energy calculations than by the reoptimization of the structures of the MP level.

I. Introduction

Results of ab initio calculations have recently been reported[1] on the two unimolecular competing reactions (dehydration and decarboxylation) occurring during the pyrolysis of formic acid. To explain the apparent inconsistency of the exptl. results, i.e., a lowest activation energy value of the decarboxylation process (48.5 kcal mol^{-1}) vs. the dehydration one (62–65 kcal mol^{-1}) and a CO/CO_2 ratio of product yield of 10, a new reaction mechanism was proposed. In particular, if the dehydration constitutes the main channel of formic acid pyrolysis, then some of the produced water molecules could serve as catalysts for the decarboxylation reaction. In this scheme, the calculated activation barriers were relatively close to the experimental values[2,3] and the observed product ratio was therefore explained by the dependence of one

(1) Ruelle, P.; Kesselring, U. W.; Hô Nam-Tran *J. Am. Chem. Soc.* **1986**, *108*, 371.

(2) Blake, P. G.; Davies, H. H.; Jackson, G. E. *J. Chem. Soc. B* **1971**, 1923.

(3) Hsu, D. S. Y.; Shaub, W. M.; Blackburn, M.; Lin, M. C. *The Nineteenth International Symposium on Combustion*; The Combustion Institute: Pittsburgh, 1983; p 89.

0002-7863/87/1509-1722$01.50/0

Table I. Ab Initio Optimized Structures of the Stationary Points for the Formic Acid Decomposition (bond length in angstroms; bond angle in degrees)

molecule	parameter	6-31G	6-31G**	MP2/6-31G	MP2/6-31G**
formic acid	C1-O2	1.204	1.182	1.244	1.212
syn	C1-O4	1.345	1.321	1.391	1.349
	C1-H3	1.073	1.085	1.091	1.092
	O4-H5	0.955	0.949	0.986	0.971
	H3-C1-O2	124.9	124.7	125.9	125.4
	O4-C1-O2	124.4	124.8	124.9	125.2
	H5-O4-C1	114.9	108.9	110.9	106.0
3-center	C1-O2	1.135	1.117	1.181	1.158
transition	C1-O4	1.848	1.846	1.879	1.819
state	C1-H3	1.169	1.165	1.195	1.195
	O4-H3	1.357	1.351	1.354	1.309
	O4-H5	0.954	0.946	0.983	0.970
	O2-C1-O4	128.5	129.4	131.0	130.3
	O4-C1-H3	47.1	46.9	45.9	45.9
	H3-O4-H5	163.3	164.6	163.1	162.7
4-center	C1-O2	1.154	1.147	1.205	1.184
transition	C1-O4	1.271	1.235	1.313	1.268
state	C1-H3	1.559	1.454	1.509	1.421
	O4-H5	1.276	1.259	1.345	1.308
	H3-H5	1.076	1.023	1.067	1.005
	O4-C1-O2	150.7	149.1	145.8	147.0
	H3-C1-O4	91.7	97.2	94.9	99.4
	C1-O4-H5	76.9	70.1	72.8	66.8
	C1-H3-H5	71.3	68.1	73.3	69.1
	H3-H5-O4	120.1	124.5	119.1	124.7
6-center	C1-O2	1.192	1.169	1.230	
transition	C1-O4	1.227	1.207	1.279	
state	C1-H3	1.409	1.411	1.399	
	O4-H5	1.865	1.719	1.593	
	H5-O6	0.967	0.976	1.035	
	O6-H8	0.947	0.949	0.974	
	O6-H7	1.157	1.142	1.183	
	H3-H7	1.052	1.071	1.084	
	O4-C1-O2	144.4	144.7	141.4	
	O4-C1-H3	108.2	109.0	108.2	
	C1-O4-H5	114.1	110.8	109.5	
	O4-H5-O6	118.8	133.1	138.8	
	H5-O6-H7	106.0	93.3	95.1	
	O6-H7-H3	158.0	160.9	149.1	
	C1-H3-H7	114.8	112.5	119.1	
	H5-O6-H8	122.5	110.1	118.0	
	H8-O6-H5-O4	166.7	110.7	127.2	
CO_2	C-O	1.161	1.143	1.205	1.179
H_2	H-H	0.730	0.732	0.737	0.734
H_2O	O-H	0.949	0.943	0.974	0.961
	H-O-H	111.6	106.0	109.3	103.8
CO	C-O	1.131	1.114	1.177	1.150

of the two processes on the other one.

Nevertheless, these reactions need for further theoretical investigations. The structures of all the stationary points located on the reaction pathways were only optimized at the SCF level and were then used to calculate the activation barriers and reaction energies, including the valence electron correlation effects in the frame of the Møller–Plesset (MP) perturbation theory. At that time, it was suggested that both the values of the geometrical parameters of the stationary points and the activation barriers, in particular for the dehydration process, could still be improved by performing geometry optimizations at the MP level of calculation. Thus, it was decided to reexamine at this level the dehydration and decarboxylation reactions of formic acid.

II. Computational Methods

A number of theoretical models were employed throughout this work which can be differentiated by the flexibility of the basis sets (6–31G[4] and 6-31G**[5]) and by the level or order of perturbation theory used both in the geometry optimizations and for single-point calculations. The correlation technique used here is Møller–Plesset perturbation theory (MP)[6] terminated at second (MP2), third (MP3), or fourth (MP4) order. With respect to the previous computations,[1] all electrons were included at the different orders of perturbation, and MP4 was treated so far as in the space of single, double, triple, and quadruple substitutions, i.e., MP4SDTQ, relative to a closed shell HF wave function. All calculations were performed with the GAUSSIAN-82 program[7] on a VAX 8600 Digital computer.

III. Results and Discussion

As discussed in the previous paper, the two reaction mechanisms occurring in the pyrolysis of formic acid above 670 °C are described by eight stationary points located on the potential energy hypersurface (Figure 1): the syn HCOOH conformer (the anti

(4) Hehre, W. J.; Ditchfield, R.; Pople, J. A. *J. Chem. Phys.* **1972**, *56*, 2257.

(5) Hariharan, P. C.; Pople, J. A. *Theor. Chim. Acta* **1973**, *28*, 213.

(6) Møller, C.; Plesset, M. *Phys. Rev.* **1934**, *46*, 618.

(7) Binkley, J. S.; Frisch, M. J.; DeFrees, D. J.; Raghavachari, K.; Whiteside, R. A.; Schlegel, H. B.; Fluder, E. M.; Pople, J. A. *Program Gaussian-82*; Carnegie-Mellon University: Philadelphia, PA 1983.

Table II. Relative Energies for the Formic Acid Dehydration Reaction (kcal mol^{-1})

method	E^{act}	ΔE^{react}	method	E^{act}	ΔE^{react}
HF/STO-3G//HF/STO-3G	117.98	16.65			
HF/3-21G//HF/STO-3G	90.54	12.58			
HF/3-21G//HF/3-21G	85.00	13.14			
HF/4-31G//HF/4-31G	82.60	9.17			
HF/6-31G//HF/6-31G	82.34	8.10	HF/6-31G//MP2/6-31G	82.22	8.05
MP2/6-31G//HF/6-31G	67.53	8.02	MP2/6-31G//MP2/6-31G	67.62	8.12
MP3/6-31G//HF/6-31G	76.18	11.12	MP3/6-31G//MP2/6-31G	77.38	12.19
MP4DQ/6-31G//HF/6-31G	73.60	8.62	MP4DQ/6-31G//MP2/6-31G	74.21	9.00
MP4SDQ/6-31G//HF/6-31G	70.73	8.02	MP4SDQ/6-31G//MP2/6-31G	70.76	7.96
MP4SDTQ/6-31G//HF/6-31G	66.56	7.43	MP4SDTQ/6-31G//MP2/6-31G	65.83	6.88
HF/6-31G**//HF/6-31G**	93.32	5.69	HF/6-31G**//MP2/6-31G**	94.02	6.15
MP2/6-31G**/HF/6-31G**	80.95	13.12	MP2/6-31G**//MP2/6-31G**	80.15	12.72
MP3/6-31G**//HF/6-31G**	87.01	11.40	MP3/6-31G**//MP2/6-31G**	87.02	11.58
MP4DQ/6-31G**//HF/6-31G**	85.67	9.80	MP4DQ/6-31G**//MP2/6-31G**	85.44	9.68
MP4SDQ/6-31G**//HF/6-31G**	83.25	10.04	MP4SDQ/6-31G**//MP2/6-31G**	82.73	9.66
MP4SDTQ/6-31G**//HF/6-31G**	79.62	10.84	MP4SDTQ/6-31G**//MP2/6-31G**	78.71	10.19
MP2(FC)/6-31G//HF/6-31G	67.50	7.96			
MP2(FC)/6-31G**//HF/6-31G**	80.69	12.63			
exptl	60–65	8.31			

conformer has not been calculated in this work), three transition states (a three-, a four-, and a six-center transition state corresponding respectively to the dehydration and the uncatalyzed and water-catalyzed decarboxylation), and four product molecules H_2O, CO, H_2, and CO_2. The MP2/6-31G and MP2/6-31G** optimized geometrical parameters of these eight stationary points are given in Table I. For the sake of comparison, the corresponding 6-31G and 6-31G** HF values are also reported in that table.

Considering first the geometries of the equilibrium structures (**1**, **5–8**), it can easily be observed that, at every level of theory, bond lengths are generally decreased when polarization functions are added to the atomic basis set. On the contrary, as shown by DeFrees et al.,[8] the correlation corrections result always in bond lengthening for each of the basis sets used. Relative to the HF/6-31G values, the MP2/6-31G** bond lengths of the equilibrium structures can thus be regarded as resulting from two opposing but not equal effects: shortening of the bond lengths by extension of the basis set and lengthening by inclusion of the MP2 corrections. As for the transition structures (**2–4**), the effect of the basis set extension are found similar in trends to those mentioned for the equilibrium structures (shorteing of the bond lengths) but the correlation effect do not operate in the same direction for all geometrical parameters. For instance, the C_1–H_3 distances in the three- and four-center transition states are respectively increased and decreased by 0.026 and 0.050 Å in going from HF/6-31G to MP2/6-31G calculations. On the other hand, although most of the bond lengths which characterize the six-membered transition state **4** are lengthened when MP2 corrections are included at the 6-31G level, the C_1–H_3 and O_4–H_5 distances are shortened by 0.010 and 0.272 Å. In all stationary points studied, Hartree–Fock bond angles are only slightly changed as a result of the inclusion of electron correlation.

More important than the actual correlation-induced changes in geometry is the effect of those changes on the relative energies of the different species encountered on the reaction pathways. The relative energies corresponding respectively to the dehydration and decarboxylation processes are given in Tables II and III. All the energies reported in those tables are relative to those of the reactant, i.e., the syn formic acid conformer **1**.

A comparison between the values based on HF and MP2 geometries shows clearly that, for either process, the correlation-induced geometry differences lead to only very small variations in both barrier heights and reaction energies. The energy differences are typically less than 1 kcal mol^{-1} although the geometry changes are quite large. It may then be concluded that high level

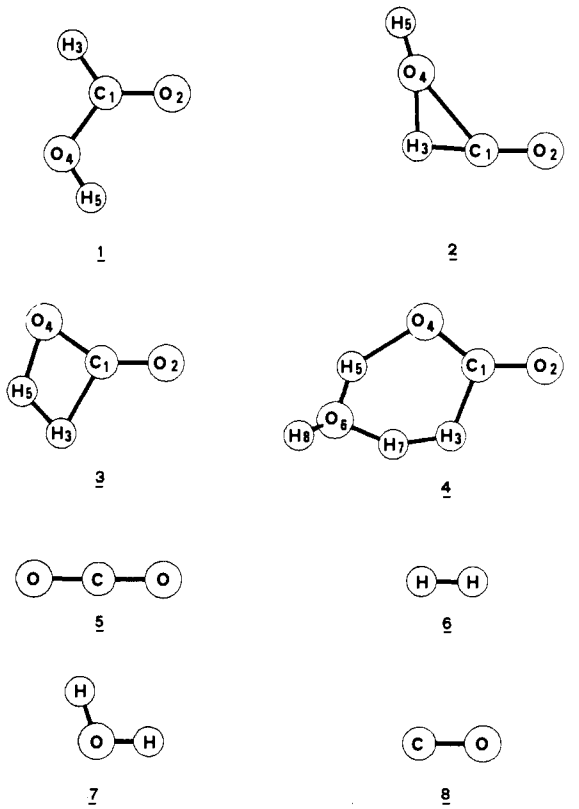

Figure 1. ORTEP plots of the stationary points that are relevant in the study of the formic acid pyrolysis.

geometry optimizations with correlated wave functions are necessary only for calculations where very high accuracy is required. From Figure 2 which reports the graphic representation of the barrier heights given in Tables II and III vs. the level of theory, it appears that the choice of an adequate basis set and the correlation corrections evaluated by single-point calculations are far more important than reoptimization of the structure at the MP level. As can be seen in Figure 2, each reaction mechanism presents its own dependence on the polarization and correlation effects which in some cases cancel each other. For the dehydration process, for instance, it is clear that the inclusion of polarization functions at any level of theory increases significantly the activation barrier of the reaction, which is then decreased by the correlation effects. In this case, the HF/6-31G//HF/6-31G barrier height (82.3 kcal mol^{-1}) does not greatly differ from the MP4SDTQ/

(8) DeFrees, D. J.; Levy, B. A.; Pollack, S. K.; Hehre, W. J.; Binkley, J. S.; Pople, J. A. *J. Am. Chem. Soc.* **1979**, *101*, 4085.

Table III. Relative Energies for the Formic Acid Decarboxylation Reaction (kcal mol^{-1})

method	E^{act}	E_{H2O}^{act}	ΔE^{react}	method	E^{act}	E_{H2O}^{act}	ΔE^{react}
HF/STO-3G//HF/STO-3G	131.80	76.66	20.07				
HF/3-21G//HF/STO-3G	108.64	59.36	10.54				
HF/3-21G//HF/3-21G	106.44	54.99	10.03				
HF/4-31G//HF/4-21G	112.70	65.97	13.05				
HF/6-31G//HF/6-31G	114.44	68.01	14.89	HF/6-31G//MP2/6-31G	115.12	68.94	15.96
MP2/6-31G//HF/6-31G	88.91	47.79	−4.42	MP2/6-31G//MP2/6-31G	88.10	46.99	−5.54
MP3/6-31G//HF/6-31G	94.35	57.47	7.46	MP3/6-31G//MP2/6-31G	99.92	56.95	8.44
MP4DQ/6-31G//HF/6-31G	97.21	56.63	4.82	MP4DQ/6-31G//MP2/6-31G	97.31	56.09	5.09
MP4SDQ/6-31G//HF/6-31G	93.52	53.29	1.78	MP4SDQ/6-31G//MP2/6-31G	92.61	52.42	1.04
MP4SDTQ/6-31G//HF/6-31G	87.48	47.47	−4.96	MP4SDTQ/6-31G//MP2/6-31G	85.44	46.21	−7.35
HF/6-31G**//HF/6-31G**	95.98	67.83	3.17	HF/6-31G**//MP2/6-31G**	96.75		4.68
MP2/6-31G**//HF/6-31G**	77.59		−1.85	MP2/6-31G**//MP2/6-31G**	76.71		−3.22
MP3/6-31G**//HF/6-31G**	85.34		4.47	MP3/6-31G**//MP2/6-31G**	85.41		4.62
MP4DQ/6-31G**//HF/6-31G**	84.68		3.47	MP4DQ/6-31G**//MP2/6-31G**	84.52		3.29
MP4SDQ/6-31G**//HF/6-31G**	81.97		1.64	MP4SDQ/6-31G**//MP2/6-31G**	81.29		0.84
MP4SDTQ/6-31G**//HF/6-31G**	77.31		−1.99	MP4SDTQ/6-31G**//MP2/6-31G**	75.97		−3.86
MP2(FC)/6-31G//HF/6-31G	88.90	47.83	−4.44				
MP2(FC)/6-31G**//HF/6-31G**	77.61	48.70	−1.65				
exptl		48.5 65–68	−1.36				

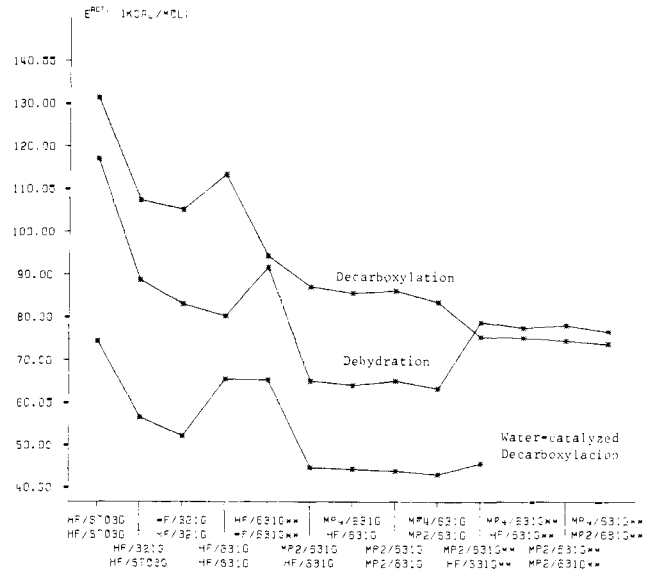

Figure 2. Variation of the barrier heights of the dehydration and decarboxylation reactions of formic acid vs. the level of theory.

6-31G**//HF/6-31G** values (79.6 kcal mol^{-1}). On the other hand, a reverse behavior is observed for the uncatalyzed decarboxylation mechanism where both the addition of polarization functions and the inclusion of the electron correlation decrease the activation barrier. A decrease as large as 37.1 kcal mol^{-1} of the relative energy is obtained in going from HF/6-31G//HF/6-31G calculations to MP4SDTQ/6-31G**//HF/6-31G** calculations. As for the third mechanism studied in this work which must correspond to the effective decarboxylation mechanism in the formic acid pyrolysis, the values of the barrier heights vary still differently than those of the two previous processes. The activation barrier is not modified at the SCF level by the introduction of the polarization functions into the DZ atomic basis set.

According to these observations, it seems on the one hand difficult to foresee, in absence of any calculation, how the barrier heights would be altered by further basis set improvements. On the other hand, it may be dangerous to transpose to any chemical process the basis set and electron correlation effects observed for a particular reaction mechanism. More constant perhaps from one reaction to another is the variation of the activation barriers with the order of the Møller–Plesset expansion. For the three mechanisms considered, similar trends are observed. In all cases, the MP2 barrier heights were less than 2 kcal mol^{-1} higher than those calculated at the MP4SDTQ level; the MP3 or incomplete MP4 treatments of correlation energies lead to underestimations of the correlation corrections. In particular, from the values tabulated in Tables II and III, it clearly appears that the barrier heights obtained with a fourth-order perturbation treatment taking into account of only the single, double, and quadruple excitations are underestimated by 3–5 kcal mol^{-1} with respect to the values derived from a full MP4 expansion.

Finally, let us note that the inclusion of all the electrons in the Møller–Plesset perturbation treatment instead of only the valence electrons does not improve the barrier heights.

IV. Conclusion

Calculations including electron correlation effects on both the geometries and energies of the different stationary points encountered along the dehydration and decarboxylation pathways of formic acid have been reported. The analysis of the results has shown that MP2 calculations based on HF optimized geometries are expected to introduce errors of only a few kcal mol^{-1} in the activation barriers.

Acknowledgment. This work is part of the project funded by the Swiss National Foundation for Scientific Research (Grant No 3.654-0.84). The author gratefully acknowledges the Département de Mathématiques de l'Ecole Polytechnique Fédérale de Lausanne for the generous allowance of computer time.

Registry No. HCO_2H, 64-18-6.